The sodium leak channel NALCN encodes the major background sodium ion conductance in murine anterior pituitary cells

Marziyeh Belal[1&2*], Mariusz Mucha[1], Arnaud Monteil[3], Paul G Winyard[4], Robert Pawlak[1], Jamie J. Walker[5,6&7],Joel Tabak[1*], Mino D C Belle[1*].

[1] University of Exeter Medical School, Hatherly Labs, Streatham Campus, Prince of Wales Road, Exeter, Devon, UK.

[2] Northwestern University, Feinberg School of Medicine, Chicago, IL 60611, United States.

[3] IGF, University of Montpellier, CNRS, INSERM, Montpellier, France.

[4] University of Exeter Medical School, St Luke's Campus, Exeter EX1 2LU

[5] College of Engineering, Mathematics and Physical Sciences, University of Exeter, Exeter, UK.

[6] EPSRC Centre for Predictive Modelling in Healthcare, University of Exeter, Exeter, UK.

[7] Bristol Medical School, Translational Health Sciences, University of Bristol, Bristol, UK.

Abstract

The pituitary gland, the so-called "master gland" produces and secretes a variety of hormones essential for regulating growth and development, metabolic homeostasis, reproduction and the stress response. The interplay between the brain and peripheral feedback signals controls hormone secretion from pituitary cells by regulating the properties of ion channels, and in turn, cell excitability. Endocrine anterior pituitary cells fire spontaneous action potentials to regulate their intracellular calcium level and eventually hormone secretion. However, the molecular identity of the non-selective cationic leak channel involved in maintaining the resting membrane potential at the firing threshold remained unknown. Here, we show that the sodium leak channel NALCN, known to modulate neuronal excitability, also regulates excitability in murine anterior pituitary cells. Using viral transduction combined with electrophysiology and

calcium imaging we show that NALCN encodes the major Na^+ leak conductance which tunes the resting membrane potential close to firing threshold to sustain the intrinsically-regulated firing in endocrine pituitary cells. Genetic interruption of NALCN channel activity, hyperpolarised the membrane potential drastically and stopped the firing activity and consequently abolished the cytosolic calcium oscillations. Moreover, we found that NALCN conductance forms a very small fraction of the total cell conductance yet has a profound impact on modulating pituitary cell excitability. Taken together, our results demonstrate that, NALCN is a crucial regulator of pituitary cell excitability and supports spontaneous firing activity to consequently regulate hormonal secretion. Our results suggest that receptor-mediated and potentially circadian changes in NALCN conductance can powerfully affect pituitary activity and hormone secretion.

Introduction

The electrical activity of cells, in response to external inputs or intrinsically derived stimulation, drives physiological functions that are essential to life, such as breathing, heartbeat, and hormone release (Cui et al, 2016; Protze et al, 2017; Rorsman and Ashcroft, 2018; Bertram et al 2018). This electrical activity relies on depolarising conductances acting on the cellular membrane to maintain the resting membrane potential (RMP) near firing threshold, driving cells to discharge action potentials (APs). In hormone-secreting cells of the pituitary gland, spontaneous electrical activity results in rhythmic Ca^{2+} entry through voltage-gated calcium channels. The subsequent oscillations in cytosolic calcium concentration ($[Ca^{2+}]_i$) serve a plethora of key physiological purposes, such as triggering hormone secretion, maintaining Ca^{2+} levels within intracellular calcium stores, and regulating gene expression (Mollard & Schlegel, 1996; Kwiecien & Hammond, 1998; Stojilkovic, 2012). Silencing spontaneous firing in pituitary cells immediately abolishes $[Ca^{2+}]_i$ oscillations and basal hormone secretion (Kucka et al, 2010).

The ability of pituitary cells to produce spontaneous APs is in part due to the depolarised RMP relative to the K^+ equilibrium potential (Fletcher et al, 2018).

Replacing extracellular Na^+ with large impermeable cations such as $NMDG^+$ immediately suppresses the cell's ability to become depolarised. Instead, hyperpolarises the RMP, silences firing activity and abolishes the $[Ca^{2+}]_i$ transients (Simasko, 1994; Sankaranarayan & Simasko, 1996; Kwiecien and Hammond, 1998; Tsaneva-Atanasova et al, 2007; Kucka et al, 2010, 2012; Tomic et al, 2011; Liang et al, 2011; Zemkova et al, 2016; Kayano et al, 2019). This reflects the presence of constitutively-active inward-depolarising currents in pituitary cells that set the membrane potential close to the firing threshold. Pharmacological and electrophysiological investigation of this inward leak current indicate that it is mediated by a TTX-insensitive, voltage-independent and constitutively active Na^+-permeable conductance (Fletcher et al, 2018).

Whilst the molecular identity of this resting Na^+ conductance in pituitary cells remains unknown, the Na^+ leak channel/nonselective (NALCN) has emerged as the major background Na^+-permeable conductance in several neuronal populations. For example, NALCN is essential for maintaining the spontaneous generation of action potentials in hippocampal neurons (Lu et al, 2007), GABAergic and dopaminergic neurons of the midbrain (Lutas et al, 2016; Philippart and Khaliq, 2018) and neurons of the suprachiasmatic nucleus of the hypothalamus (Flourakis et al, 2015). In ventral respiratory neurons of the brain stem, NALCN facilitates rhythmic and CO_2 stimulated breathing, as well as responsiveness to neuropeptides (Lu et al, 2007; Shi et al, 2016; Yeh et al, 2017).

The importance of NALCN as a regulator of electrical responsiveness in endocrine cells such as pancreatic β cells, is also emerging (Swayne et al 2009). A high level of NALCN mRNA expression in the pituitary gland has been reported (Swayne et al, 2009). Further, transcriptomic data indicated that every anterior pituitary cell type significantly expresses NALCN and its known regulatory subunits (UNC-79, UNC-80, FAM155A) at levels higher than other known cationic leak channel, such as TRP channels and HCN channels (Paul Le Tissier, Jacques Drouin and Patrice Mollard, personal communication, 04/2021). Moreover, NALCN has recently been shown to regulate cell excitability in a pituitary clonal cell line (Impheng et al, 2021). Finally, the pharmacological profile of NALCN in neurons is similar to that of resting Na^+

conductance in pituitary cells: TTX-insensitive, extracellular Ca^{2+}- and $NMDG^{+}$-sensitive.

Together, this strongly suggests that NALCN is the primary contributor to the background Na^{+} conductance and consequently plays a key role in regulating cell excitability in pituitary cells. To test this, we used a lentiviral-mediated knockdown strategy combined with electrophysiology and calcium imaging to evaluate the role of NALCN in regulating the electrical and $[Ca^{2+}]_i$ activity of murine primary anterior pituitary cells. This multifaceted approach not only allowed us to determine that NALCN is the main contributor to the background Na^{+}-permeable conductance of pituitary cells but also enabled us to estimate the magnitude of this conductance.

Results

Primary murine anterior pituitary cells express NALCN channel protein

Previous research revealed the expression of *Nalcn* gene in mouse anterior pituitary gland at the mRNA level (Swayne et al, 2009). Thus, we first confirmed the expression of NALCN protein in primary endocrine pituitary cells. Using fluorescence immunohistochemistry and the use of NALCN antibody directed at the extracellular epitope of NALCN protein, we could detect the presence of NALCN channel in murine endocrine anterior pituitary cells (Figure 1). Here, the majority of the anterior pituitary cells were stained with the NALCN antibody, and no staining was observed when the primary NALCN antibody was omitted (Figure 1H).

NALCN regulates spontaneous firing of primary pituitary cells

Given that gadolinium (Gd^{3+}) and flufenamic acid (FFA) block the spontaneous firing of pituitary cells (Kucka et al, 2012) and thus revealing the presence of a functional non-selective cationic conductance (NSCC), it is noteworthy that Gd^{3+} and FFA are not specific blockers of a particular non-selective cationic conductance. Thus, NSCCs other than NALCN may contribute to the effects of FFA and Gd^{3+} on membrane potential. To determine if NALCN is the main NSCC in endocrine anterior pituitary cells, we used a genetic manipulation approach to directly investigate the role of NALCN in the regulation of spontaneous firing in these cells. We set up a lentiviral-mediated knockdown

strategy to decrease NALCN expression level, and then evaluated the resulting changes in electrophysiological properties of pituitary cells.

Most untreated control (untreated Ctrl) and scramble control (SCR Ctrl) cells exhibited spontaneous firing activity (Figure 2A,B,D,F), consistent with the previous reports (*reviewed in* Fletcher et al, 2018). In contrast, 90% (28 of 31) of NALCN knockdown (NALCN KD) cells were found to be silent (Figure 2C,D,F), compared to just 17% (5 of 30) in SCR control and 19% (6 of 31) in untreated control cells (Figure 2D,F). In addition, NALCN KD cells exhibited a significantly more hyperpolarised resting membrane potential (RMP) compared to both untreated and SCR control cells (NALCN KD RMP: -63.6 ± 8.5 mV (mean ± SD), n=31 from 12 animals; SCR Ctrl: -45.2 mV ± 5.8 mV, n=30, 12 animals; untreated Ctrl: -47.5 mV ± 7.8, n=31, 12 animals; $p<0.001$, one-way ANOVA with post hoc Bonferroni correction; Figure 2E). There was no significant difference between the SCR control cells and untreated control cells either for the firing frequency (untreated Ctrl: 0.7 ± 0.6 Hz, n=25; SCR Ctrl: 0.5 ± 0.4 Hz, n=25, $p>0.1$, *t*-test; Figure 2F) or for the RMP value (untreated Ctrl: -47.6 ± 7.6 mV, n=31; SCR Ctrl: -45.2 mV ± 5.8 mV, n=30 $p>0.1$, *t*-test; Figure 2E). Thus, the viral transduction *per se* did not affect the firing activity or RMP of pituitary cells. In the following sections we will therefore only compare NALCN KD cells with SCR control cells.

Small conductance injection restores firing in NALCN KD cells

We next use dynamic-clamp to examine whether the injection of nonselective cationic conductance to silent NALCN KD cells could restore spontaneous firing activity. Indeed, silent NALCN KD cells became active and gained their typical firing activity upon increasing the non-selective cationic conductance (Figure 3A). The added conductance required to bring the NALCN KD cells to fire ranged from 0.02 to 0.12 nS (median 0.05 nS, n=28, Figure 3B).

Taken together, this first set of results indicates that NALCN is a key player in pituitary cell excitability, by modulating the RMP and subsequently the firing activity of primary pituitary cells. The amount of NALCN conductance lost by the cells after NALCN KD appears to be on the order of 0.05 nS.

175

176 **NALCN contributes to the inward Na^+ leak current in primary pituitary**
177 **cells**

178 To further determine the contribution of the NALCN-mediated inward leak
179 current to the background Na^+ current of pituitary cells, we compared the inward
180 currents at a holding potential of -80 mV in SCR control and NALCN KD cells to
181 remove any influence from K^+ channel conductance. The holding current
182 obtained by voltage clamping cells at -80 mV was found to be significantly
183 larger in the SCR control group compared to the NALCN KD group (Figure 4A-
184 C, SCR control (mean ± SD): -0.72 ± 0.2 pA/pF, n=15; NALCN KD: -0.19 ± 0.13
185 pA/pF, n=16; p< 0.001, *t*-test), confirming that the NALCN KD cells were more
186 hyperpolarised. Remarkably, this background Na^+ conductance was reduced by
187 0.045 nS in SCR control, but by only 0.015 nS in NALCN KD upon the
188 substitution of extracellular Na^+ with the impermeant cation $NMDG^+$. This
189 indicates that the measured inward currents were mediated by a background
190 Na^+ conductance which was more strongly reduced in NALCN KD cells (Figure
191 4D, SCR control (median ± interquartile): 0.045 ± 0.02 nS, n = 16; NALCN KD:
192 0.015 ± 0.01 nS, n = 15; p < 0.001, Mann Whitney test).

193

194 These findings indicate that NALCN contributes most of the inward leak
195 conductance in pituitary cells. Moreover, we obtained a rough estimate of the
196 contribution of NALCN channels to the background Na^+ conductance by noting
197 that the difference in background Na^+ conductance between the SCR control
198 and NALCN KD group is 0.045 – 0.015 = 0.03 nS. This is probably an
199 underestimate since the NALCN KD may not have removed all the channels,
200 but it implies that a change in background Na^+ conductance of just 0.03 nS can
201 have a profound effect on the electrical activity of endocrine anterior pituitary
202 cells. This is in agreement with the observation that adding 0.05 nS of inward
203 leak conductance in NALCN KD cells restore electrical activity (Figure 3B).

204

205 **NALCN is required for spontaneous intracellular Ca^{2+} oscillations in**
206 **primary pituitary cells**

207 Previous studies have shown that the pattern of spontaneous firing determines
208 the amplitude and duration of intracellular Ca^{2+} oscillations in anterior endocrine
209 pituitary cells (Stojilkovic et al, 2005, Stojilkovic et al, 2012). Thus, we next

tested whether NALCN KD affects spontaneous intracellular Ca^{2+} transients in these cells. Consistent with a previous report (Tomić et al, 2011), approximately 57 % (51 of 90) of SCR control pituitary cells exhibited spontaneous intracellular Ca^{2+} transients (Figure 5A). In contrast, only 11 % (4 of 36) of NALCN KD cells displayed low-amplitude intracellular Ca^{2+} transients, the remaining 89 % were quiescent and did not generate any intracellular Ca^{2+} oscillations. (Figure 5B). To quantitatively compare the size of the intracellular Ca^{2+} fluctuations between the SCR control and NALCN KD cells, the standard deviation of the Ca^{2+} trace for each individual cell was calculated over 600 seconds. Comparing the standard deviation between the two groups revealed a statistically-significant difference (Figure 5C, SCR control: median=0.04, n=90; NALCN KD: median=0.015, n=36; $p<0.001$, Mann Whitney test). The final peak in each trace in Figure 5A,B represents the extracellular K^+ (15 mM) induced depolarisation and consequently a rise in $[Ca^{2+}]_i$, which was used as a control for the viability of cells. This indicated that NALCN plays a role in regulating intracellular Ca^{2+} oscillations of primary pituitary cells.

NALCN mediates a low extracellular Ca^{2+}-induced depolarisation in primary pituitary cells

In primary anterior pituitary cells, the lowering or removal of extracellular Ca^{2+} causes membrane depolarisation and silencing of spontaneous firing activity but with no effect on $[Ca^{2+}]_i$ (Stojilkovic, 2006; Sankaranarayanan and Simasko, 1996; Kwiecien and Hammond, 1998; Tsaneva-Atanasova et al, 2007). The removal of extracellular Ca^{2+} in hippocampal neurons activates slow and sustained inward leak currents through the NSCC (Chu et al, 2003). It is reported that the removal of extracellular Ca^{2+} activates the UNC80-NALCN complex, increasing the NALCN current and thus regulating excitability in neurons (Lu et al, 2010). Therefore, we next explored the possibility that NALCN could be responsible for the low extracellular Ca^{2+}-induced depolarisation in pituitary cells. To test this hypothesis, the inward leak current was measured at a holding potential of -80 mV before and after reducing extracellular Ca^{2+} from 2 mM to 0.1 mM.

Consistent with previous studies in neurons, removal of extracellular Ca^{2+} significantly increased the inward leak current in SCR control pituitary cells over

a time-course of 20 to 200 seconds (median ± interquartile: −0.8 ± 0.6 pA/pF to −1.5 ± 0.5 pA/pF, n = 15, p < 0.001, Kruskal-Wallis, Figure 6A,C). Subsequent replacement of extracellular Na^+ with $NMDG^+$ reduced the holding inward leak current (−1.5 ± 0.5 pA/pF to −0.3 ± 0.2 pA/pF, n = 15, p < 0.001, Kruskal-Wallis, Figure 6A,C), indicating that the extracellular Ca^{2+}-induced depolarisation is Na^+ mediated. In contrast, lowering the extracellular Ca^{2+} in NALCN KD pituitary cells results in a small rise in the inward leak current (−0.37 ± 0.35 pA/pF to −0.5 ± 0.25 pA/pF, n = 13, p < 0.05, Figure 6B,C). The substitution of extracellular Na^+ with $NMDG^+$ in NALCN KD cells still reduced the inward leak current but only marginally by comparison (−0.5 ± 0.25 pA/pF to −0.2 ± 0.25 pA/pF, n = 13, p < 0.01, Figure 6C), which reinforces the fact that NALCN is involved. This current could result from residual NALCN still expressed in the NALCN KD cells (since knocking down NALCN may not necessarily result in a 100% knock out) or contribution from other NSCCs, or from the seal conductance.

The overall rise in the inward leak current after reducing extracellular Ca^{2+} in control pituitary cells was significantly higher than that in NALCN KD pituitary cells (median ± interquartile in SCR control: −0.6 ± 0.6 pA/pF, n = 13, NALCN KD: −0.13 ± 0.1 pA/pF, n = 13, p < 0.001, Mann Whitney test, Figure 6D). Our results show that, similarly to what has been observed in neurons, NALCN current is reduced by extracellular Ca^{2+} and is involved in the low Ca^{2+}-induced depolarisation observed in pituitary cells.

Discussion

NALCN regulates the excitability of murine anterior pituitary cells

All endocrine anterior pituitary cell types produce intrinsically-regulated firing. This firing is crucial for maintaining their normal physiology such as basal hormone secretion, gene expression and Ca^{2+} stores level (Kwiecien and Hammond, 1998; Stojilkovic et al, 2010; Fletcher et al, 2018). However, the molecular identity of the major non-selective cationic conductance (NSCC) that enables spontaneous firing in pituitary cells is not fully determined (Fletcher et al, 2018). Pharmacological studies have revealed that the NSCC is unequivocally Na^+-dependent and TTX-resistant (Simasko, 1994;

Sankaranarayanan and Simasko, 1996; Kucka et al, 2010; Liang et al, 2011; Tomic et al, 2011; Zemkova et al, 2016). Some studies have suggested that transient receptor cation channels (TRPC), as well as hyperpolarisation-activated cyclic nucleotide-gated channel (HCN) may contribute to the NSCC described in pituitary cells and related cell lines (Tomic et al, 2011; Kucka et al, 2012; Kayano et al, 2019, Kretschmannova et al, 2012). However, these deductions were based on RNA expression profile as well as on the use of non-selective pharmacological compounds. In addition, no genetic manipulations (e.g. modification of the ion channel expression level) were performed to demonstrate their contribution to NSCC. A recent study, however, implicates NALCN as a major contributor to the NSCC in the GH3 pituitary cell line (Impheng et al, 2021).

To determine whether this finding extends to native pituitary cells, we applied genetic manipulation to knockdown NALCN channel, in combination with electrophysiology and calcium imaging to investigate its role in regulating cell excitability and $[Ca^{2+}]_i$ oscillations in cultured murine anterior pituitary cells. We found that 1) NALCN channel encodes a major Na^+ leak conductance to sustain the spontaneous firing activity in endocrine pituitary cells, 2) NALCN is the main contributor to the depolarising NSCC in pituitary cells, without which the cells remain silent and hyperpolarised. 3) NALCN is crucial for maintaining spontaneous intracellular Ca^{2+} transients in these cells. 4) As in neurons, NALCN activity is sensitive to the extracellular Ca^{2+} level in pituitary cells. Taken together, these results support a critical role for NALCN in both maintaining the spontaneous firing and the subsequent intracellular Ca^{2+} transients in primary pituitary cells.

We found that NALCN KD pituitary cells are significantly hyperpolarised (by about 15 mV) compared to control pituitary cells. Moreover, 90% of NALCN KD pituitary cells were entirely silent and did not generate any action potentials. Interestingly, restoring the non-selective cationic conductance in NALCN KD cells using dynamic clamp made these cells generate action potentials in the normal frequency range for pituitary cells. However, discontinuing NALCN-like conductance injection (or dynamic-clamp mimic of NALCN conductance) immediately silenced the cells, retuning the membrane potential to the

hyperpolarised state. On the other hand, in the majority of silent control pituitary cells, the removal of the NALCN-like conductance did not return them to silent state but made them sustain the normal firing (data not shown).

A small NALCN conductance sustains a large depolarising drive

The comparison between background Na^+ inward current in control cells and NALCN KD cells showed that the amount of NALCN conductance knocked down in our experiments was about 0.03 nS. This is consistent with the median 0.05 nS background Na^+ conductance required to activate silent NALCN KD cells. This dynamic clamp-based estimate does not rely on measurements of small noisy currents (a few pA) in voltage clamp, and therefore provides an estimate that is not affected by poor signal-to-noise ratio. The profound effect on electrical activity of such a small conductance results from the high input resistance of pituitary cells, on the order of 5 GΩ. Assuming a reversal potential around 0 mV for this conductance, at a membrane potential of -60 mV the current through a 0.05 nS NALCN conductance is 3 pA. If the membrane resistance is 5 GΩ, the depolarisation due to the current is therefore 15 mV. Again, this is consistent with our finding that NALCN KD cells were hyperpolarised by about 15 mV.

We have used the same knockdown approach as Impheng et al (2021), who have reported an estimated NALCN conductance of about 30 pS/pF in GH3 cells. This represents a conductance about three times larger than our estimate in native pituitary cells (10 pS/pF, given our average pituitary cell capacitance of 5 pF). We used a slightly higher extracellular concentration of Mg^{2+} than Impheng et al, 2021 (1 mM vs 0.8 mM). Given that divalent cations block NALCN (Chua et al 2020), this may explain part of the difference between our reported conductance values. It is also possible that GH3 cells simply express higher levels of NALCN. A limitation of this work is that we have not distinguished the different pituitary cell types we have recorded. Different cell types may express different average levels of NALCN. If such heterogeneity exists, then our estimate of NALCN conductance is an aggregate of the average NALCN conductance expressed by each cell-type we have sampled.

There is no available estimate for NALCN single-channel conductance, and we are probably under-estimating NALCN conductance in pituitary cells with a knockdown-based approach, since there may still be some NALCN channels expressed in the KD cells. Nevertheless, our estimate of 0.05 nS implies that cells have few active NALCN channels on their membrane. This would explain why our recordings of the non-specific cation current (Figure 4A, 6A), and others' (Liang et al 2011) are very noisy. Transient block by divalent cations, and possibly random channel gating, since NALCN has weak voltage sensitivity (Bouasse et al, 2019, Chua et al 2020), would result in relatively large current fluctuations if the number of channels is low.

NALCN activity is modulated by extracellular Ca^{2+} in pituitary cells

Under both physiological and pathological circumstances extracellular Ca^{2+} ($[Ca^{2+}]_e$) can drop markedly in various brain regions (Ren, 2011) and serum (Ferry et al, 1997). This variation of serum Ca^{2+} appears to regulate adrenocorticotropic hormone (ACTH) secretion from pituitary corticotrophs. Indeed, variations in serum Ca^{2+} within physiological range is associated with a drastic change in ACTH secretion (Isaac et al, 1984; Fuleihan et al, 1996). At the cellular level, the reduction in $[Ca^{2+}]_e$ results in membrane depolarisation of cultured rat lactotrophs and somatotrophs (Sankaranarayanan and Simasko, 1996; Tsaneva-Atanasova et al, 2007). Conversely, an increase in $[Ca^{2+}]_e$,but also in $[Mg^{2+}]_e$, to 10 mM with a concomitant blockade of calcium channel resulted in a hyperpolarisation of the membrane potential of cultured rat pituitary somatotrophs (Tsaneva-Atanasova et al, 2007). It has been speculated that the underlying mechanism of low $[Ca^{2+}]_e$ – induced membrane depolarisation could involve either the inhibition of Ca^{2+}-activated potassium channels and/or the increase of a Na^+ background conductance (Sankaranarayanan and Simasko, 1996; Tsaneva-Atanasova et *al*, 2007).

NALCN was found to be sensitive to blockade by $[Ca^{2+}]_e$ in neurons and GH3 cells (Lu et al, 2010; Bouasse et al, 2019; Impheng et al, 2021). Our results show that in mice anterior pituitary cells, NALCN channels are also sensitive to $[Ca^{2+}]_e$ blockade, and mediate the low $[Ca^{2+}]_e$-induced membrane depolarisation. Two different mechanisms have been proposed to underlie NALCN blockade by $[Ca^{2+}]_e$. First, this blockade could occur through the Ca^{2+}-

sensing receptor (CaSR) *via* a G_q-protein dependent pathway that ultimately induces NALCN phosphorylation by protein kinase C (Lu et al, 2010; Lee et al, 2019). Alternatively, this blockade could occur through direct binding of Ca^{2+} within the NALCN pore (Chua et al, 2020). It remains to determine which mechanism is involved in the NALCN modulation by $[Ca^{2+}]_e$ in primary pituitary cells. Of note, Zemkova and colleagues reported that lowering $[Ca^{2+}]_e$ had no effect on the membrane potential of corticotrophs (Zemkova et al, 2016) even though Letissier and colleagues found these cells express the NALCN-coding mRNA (personal communication). Possibly, the short amount of given time (20 seconds) during which the $[Ca^{2+}]_e$ was removed may not be long enough to allow the membrane potential to depolarise (Zemkova et al, 2016). In our experiments, the inward leak current in the majority of primary pituitary cells started to increase within 20 seconds to about a minute after removal of $[Ca^{2+}]_e$ and continued to increase within the next few minutes until it reached a steady state. This timeline suggests that a transduction cascade instead of a direct pore effect could be involved.

NALCN modulation by neurohormones: a key player in pituitary cell response to hypothalamic signals?

In addition to Ca^{2+} sensing, NALCN can be negatively and positively regulated by G-protein dependent and independent signalling pathways (Lu et al, 2009; Swayne et al, 2009; Philippart & Khaliq, 2018). We have seen above that a small NALCN conductance has a powerful effect on pituitary cell electrical excitability. Together, this suggest that NALCN modulation by hypothalamic signals would therefore provide a powerful way to control pituitary activity and regulate pituitary hormones secretion. Several studies have suggested that a NSCC is essential for facilitating pituitary cell response to hypothalamic signals. For instance, several groups have shown that hyperpolarising the cells by removing extracellular Na^+ supresses both growth hormone releasing hormone (GHRH)-induced Ca^{2+} influx (Lussier et al, 1991; Naumov et al, 1994) and GHRH-induced growth hormone secretion from rat pituitary *in vitro* (Kato et al, 1988). In the same study, it was found that TTX had no effect on either GHRH-induced GH secretion or GHRH-induced Ca^{2+} influx (Kato et al, 1988). Interestingly, it was shown that in the absence of extracellular Na^+, changing the resting membrane potential by increasing the extracellular K^+ to 15 or 30 mM

completely rescued the GHRH-induced GH secretion (Kato et al, 1988). Removal of extracellular Na^+ also substantially delayed the stimulatory response to corticotrophin-releasing hormone (CRH) by approximately 13 minutes in murine corticotroph cells (Liang et al, 2011). Consistent with these observations, Tomić et al, (2011) found that after removal of bath Na^+, stimulating adenylyl cyclase with forskolin (adenylyl cyclase and protein kinase A activator) does not rescue spontaneous $[Ca^{2+}]_i$ transients in pituitary cells.

These experiments suggest a critical role of NALCN in the response of pituitary cells to hypothalamic neurohormones. However, since these experiments essentially removed the depolarising component of NALCN, they cannot be used to assess whether NALCN is activated directly by neurohormones. In other words, the experiments cannot distinguish whether NALCN acts permissively to enable cells to respond to neurohormones or is directly involved in mediating the effects of the hormones. Thus, it could be of value to explore the impact of hypothalamic neurohormones on NALCN channel in each anterior pituitary cell type to identify the key effector ion channels involved in the regulation of pituitary hormone secretion.

The approach based on NALCN knockdown and electrophysiology developed here outlines a way to make this distinction. For example, NALCN depolarising current can be reintroduced using dynamic clamp in NALCN KD cells. In this way, while the native NALCN channel is prevented to directly mediate the action of neurohormones, its permissive action on membrane potential will be conserved. Alterations of cellular response to neurohormones under these circumstances imply that NALCN participates directly in receptor-mediated response to neurohormones.

Perspectives

Our data demonstrates that, as in neurons, NALCN is a crucial player in pituitary cell excitability by conducting a Ca^{2+}-sensitive background Na^+ conductance that regulates membrane potential. Our data thus suggests that NALCN plays a key role in regulating hormone secretion from pituitary cells. Our approach of combining NALCN knockdown and dynamic clamp can now be used to determine whether NALCN directly participates in mediating pituitary responses to hypothalamic signals. The development of *Nalcn* knockout mouse

in a specific population of anterior pituitary cells is now required to examine the impact of NALCN on the different pituitary hormones.

Materials and Methods

Primary cell culture

Murine endocrine anterior pituitary cell cultures were prepared between 8:00 and 11:00 AM from wild-type C57BL/6J mice as required. Mice were kept in groups of two to four under standard circumstances at the University of Exeter (UK) animal unit: Lights on at 6:00 AM, lights off at 6:00 PM at 21°C, tap water and food were available *ad libitum*. The adult mice aged between two to six months were selected randomly regardless of their sex. All the animal work was carried out according to the standards of the Home Office (England) and the University of Exeter. Three or four mice were culled via cervical dislocation and then were decapitated in accordance with Schedule 1 procedures. After removing the brain, the pituitary gland was removed from the sella turcica (bony cavity) and placed in a 100x21 mm culture dish (Thermo Fisher Scientific, UK) containing 150 µL 4°C DMEM (Dulbecco's modified Eagle's medium with high glucose and 25mM HEPES from Sigma Aldrich (Merck), UK) located on ice. Under a dissection microscope, the intermediate and posterior lobes were removed using a scalpel blade (size 10), and the anterior lobes were chopped to small pieces manually. Subsequently, the chopped tissues were transferred into a 50 mL falcon tube containing 2.5 mL DMEM supplemented with 207 TAME Units/mL trypsin and 36 Kunitz Units/mL DNase I (both from Sigma Aldrich, UK), and then incubated in 37°C water bath for 10 minutes. Every 5 minutes, the tube was swirled to disperse the tissue pieces evenly to achieve a thorough digestion. After 10 minutes, the suspension was gently triturated 20-30 times using a 1 mL pipette tip. At the end of the digestion step, an inhibition solution containing 5 mL DMEM supplemented with 0.25 mg/mL Lima soybean trypsin inhibitor, 100 kallikrein unit aprotinin and 36 Kunitz Units/ml DNase I (Sigma Aldrich, UK) was added to the digestion solution, and the cell

suspension was left for a few minutes to inactivate the trypsin enzyme activity. The resulting suspension was finally filtered through a cell strainer with 70 µm nylon mesh (Merck) and was centrifuged at 100×g for 10 minutes. The pellet was resuspended in 500-600 µL DMEM solution and then 60 µL was plated on each 15 mm diameter round coverslip (Thermo Fisher Scientific, UK) in a 12-well plate. After 20 minutes, once the cells were securely attached to the bottom of coverslips, 1 mL of growth medium (DMEM + 2.5% FBS + 0.1 % Fibronectin + 1% antibiotic-penstrep, from Sigma Aldrich, UK) was added to each well and then incubated at 37°C in a 5% CO_2 incubator. The culture medium was replaced with antibiotic-free growth-medium 6 hours later. The growth medium was refreshed every two days. 5 µL concentrated suspension of lentivirus was added to the medium in each well of a 12-well plate. Fresh growth medium was substituted 24 hours after transduction. Green fluorescence cells were usually observable 2-3 days after transduction and selected for electrophysiological recording. Each batch of primary pituitary cell culture was utilized for up to 5 days after transduction for electrophysiological recordings and calcium imaging.

Lentivirus

A microRNA-adapted shRNA based on miR-30 for specific NALCN silencing cloned in the lentiviral pGIPZ plasmid and targeting the 5'-GCAACAGACTGTGGCAATT-3' region of the rat NALCN-encoding RNA was obtained from a commercial source (Dharmacon #V2LMM_90196). A non-silencing scramble control was used in our experiments (Dharmacon #RHS4346). HpaI/BamHI are the restriction sites in pGIPZ plasmid between which the NALCN silencing shRNA was inserted.

Electrophysiological recording

Electrophysiological recordings from pituitary cells were performed at room temperature using single-cell amphotericin-perforated patch-clamp technique. The recordings were obtained using an Axopatch 700B amplifier and Clampex 10.1 (Molecular Devices) with a sampling rate of 10 kHz and filtered at 2 kHz (lower pass). Patch pipettes were fabricated from borosilicate glass with filament (outer diameter: 1.50 mm and inner diameter: 0.86 mm, Warner Instrument-multi channel system distributer) and pulled using a micropipette puller (Sutter Instruments, model P-97). Pipette tips were then fire polished and

had a resistance ranging from 4 to 6 MΩ. Once a high resistance seal was formed (>10 GΩ), usually within 10 minutes of patching, the access resistance (or series resistance) would reduce to less than 50 MΩ, and then recording started. If the seal resistance was less than 10 GΩ, the cell was discarded. In current clamp mode, series resistance was compensated by Bridge-Balance and was usually less than 40 MΩ. Junction potential was not corrected. In voltage clamp mode, compensated series resistance (60%) was normally less than 50 MΩ and the capacitance of recorded pituitary cells ranged between 4 and 6 pF (electronic compensation was done *via* whole-cell mode of multiclamp 700B). During recording, the cells were constantly perfused using a gravity-driven perfusion system, with a flow rate of 0.5 mL/min with extracellular solution containing (in millimolar) 138 NaCl, 5 KCl, 10 alpha-D-glucose, 25 HEPES, 0.7 Na_2HPO_4, 1 $MgCl_2$ and 2 $CaCl_2$. The pH was adjusted to 7.4 with NaOH, and the osmolality was 305 mOsmol/L. Patch pipettes were filled with an intracellular solution containing (in millimolar) 10 NaCl, 100 K-Gluconate, 50 KCl, 10 HEPES, and 1 $MgCl_2$. The pH was adjusted to 7.2 with KOH, 295 mOsmol/L. The osmolality of the solutions was maintained by adding an inert ingredient sucrose. 5 µl Amphotericin-B of a stock solution (20 mg/mL in dimethyl sulfoxide) was added to 1 mL of pipette solution to achieve a final concentration of 50 µg/ml. Other concentrations such as 10 µl Amphotericin-B were also tried, however 5 µl resulted in more durability of the recording (all salts and Amphotericin-B were purchased from Sigma Aldrich.

Dynamic clamp

With dynamic clamp we can effectively change the biophysical property of ion channels (such as activation, inactivation, gating kinetics and conductances) as we choose and investigate how these manipulations affect the pattern of electrical activity in real time. In other words, we can establish the contribution of a type of ion channel to regulating various aspects of electrical activity (Milescu et al, 2008).

In this study, a second computer and an analogue-to-digital acquisition card (DAQ) were installed to run the dynamic clamp module in the software QuB (Milescu et al, 2008). In the current clamp mode of the Axopatch 700B amplifier, the membrane potential (Vm) of a patched cell was recorded in real time and

passed to the computer running QuB as an input for a mathematical expression of non-selective cationic leak channels : $I_{NS}=g_{NS}$ (Vm - E_{NS}) which defines the corresponding current (I_{NS}) going through them. The sodium leak conductance (g_{NS}) was changed manually. The calculated I_{NS} was then injected back to the cell via the same DAQ and then the membrane voltage response was recorded. Thus, the injected NALCN-like current is varied dynamically, unlike conventional current clamp in which the injected current is constant across all time points.

The reversal potential (E_{NS}) for this channel was considered zero since this channel is permeable to different monovalent cations (e.g. K^+ and Na^+) but primarily to Na^+ (Lu et al, 2007; Chua et al, 2020).

Measurement of cytosolic calcium in single pituitary cells

The coverslips with pituitary cells were bathed in the extracellular solution (containing same ingredients as described in the above electrophysiology section) with 2µM fura-2 AM (Thermo Fischer Scientific-# F1221) for 45 minutes at 37°C. The cells were then rinsed three times with the extracellular solution using a 2 mL Pasteur pipette. Following this, the coverslips were mounted onto the recording chamber (volume ~ 0.2 mL) on the stage of an inverted microscope (Nikon eclipse Ti). Cells were constantly perfused with the extracellular solution at room temperature using a gravity-driven perfusion system. Cells were excited every 1 second with alternating 340-nm and 380-nm light beams (20 millisecond exposure time) originating from a Lambda DG-4 wavelength switcher (Sutter Instrument Company). Light intensity was reduced by 50% before hitting the cells using an appropriate filter. The intensity of emitted light was measured at 520 nm and images were acquired by a Hamamatsu digital camera C1344 set to 4 × 4 binning. Hardware control was achieved by TI Workbench software developed by T. Inoue (As used by Tabak et al, 2010). Using this software, regions of interest (ROI) were selected around the cells that were not overlapping with other cells and a single background ROI was selected in an empty space. Pixel values within each region of interest were averaged for both 340 and 380 excitation wavelengths and then subtracted from the background. Following this, a ratio (*r)* was computed according to the formula:

$r = (ROI_{340} - ROI_{background340})/ (ROI_{380} - ROI_{background380})$

Trace analysis was performed in MATLAB.

Immunohistochemistry

Pituitary glands were extracted and fixed overnight in 4% PFA in PBS. The following day, 70 µm thick sections were cut using a vibratome (Campden Instruments, UK), placed on poly-L-Lysine coated microscope slides (VWR) and left to dry. Next, the sections were blocked with 10% FBS in PBST (PBS containing 0.01% Triton X-100) for one hour at room temperature. Primary rabbit anti-NALCN antibody at 1:500 dilution (Alomone Labs, Israel, #ASC-022) in 10% FBS/PBST was applied to the sections and incubated in humid chamber at 4 C° degrees overnight. The next day, sections were washed 3 times for 15 min with PBST. Then, the secondary 488-Alexa-Fluor conjugated antibody (at 1:1000, Molecular Probes) was applied in 10% FBS/PBST solution for 1 hour at room temperature, followed by a series of three 15 min washes with PBST. The nucleic acids present in the pituitary gland cells were visualised with TOTO-3 (1:2000, Thermo Fisher Scientific). Sections were incubated with TOTO-3 for 15 min on an agitated surface, then washed three times (each time 10 min) and subsequently mounted with Fluorsave medium (Calbiochem). The controls were the sections where primary antibody was omitted. Images were obtained using a Zeiss LSM 5 Exciter confocal microscope run by Zen software.

Statistics

The type of statistical test used in each case is specified in the result using MATLAB.

References

Bertram, R., Satin, L.S., Sherman, A.S., 2018. Closing in on the Mechanisms of Pulsatile Insulin Secretion. Diabetes 67, 351–359. https://doi.org/10.2337/dbi17-0004

Bouasse, M., Impheng, H., Servant, Z., Lory, P., Monteil, A., 2019. Functional expression of CLIFAHDD and IHPRF pathogenic variants of the NALCN channel in neuronal cells reveals both gain- and loss-of-function properties. Sci. Rep. 9, 11791. https://doi.org/10.1038/s41598-019-48071-x

Chu, X., Zhu, X., Wei, W., Li, G., Simon, R.P., MacDonald, J.F., Xiong, Z., 2003. Acidosis decreases low Ca^{2+} -induced neuronal excitation by inhibiting the activity of calcium-sensing cation channels in cultured mouse hippocampal neurons. J. Physiol. 550, 385–399. https://doi.org/10.1113/jphysiol.2003.043091

Chua, H.C., Wulf, M., Weidling, C., Rasmussen, L.P., Pless, S.A., 2020. The NALCN channel complex is voltage sensitive and directly modulated by extracellular calcium. Sci. Adv. 6, eaaz3154. https://doi.org/10.1126/sciadv.aaz3154

Cui, Y., Kam, K., Sherman, D., Janczewski, W.A., Zheng, Y., Feldman, J.L., 2016. Defining preBötzinger Complex Rhythm- and Pattern-Generating Neural Microcircuits In Vivo. Neuron 91, 602–614. https://doi.org/10.1016/j.neuron.2016.07.003

Ferry, S., Chatel, B., Dodd, R.H., Lair, C., Gully, D., Maffrand, J.-P., Ruat, M., 1997. Effects of Divalent Cations and of a Calcimimetic on Adrenocorticotropic Hormone Release in Pituitary Tumor Cells. Biochem. Biophys. Res. Commun. 238, 866–873. https://doi.org/10.1006/bbrc.1997.7401

Fletcher, P.A., Sherman, A., Stojilkovic, S.S., 2018. Common and diverse elements of ion channels and receptors underlying electrical activity in endocrine pituitary cells. Mol. Cell. Endocrinol. 463, 23–36. https://doi.org/10.1016/j.mce.2017.06.022

Flourakis, M., Kula-Eversole, E., Hutchison, A.L., Han, T.H., Aranda, K., Moose, D.L., White, K.P., Dinner, A.R., Lear, B.C., Ren, D., Diekman, C.O., Raman, I.M., Allada, R., 2015. A Conserved Bicycle Model for Circadian Clock Control of Membrane Excitability. Cell 162, 836–848. https://doi.org/10.1016/j.cell.2015.07.036

Fuleihan, G.E., Brown, E.M., Gleason, R., Scott, J., Adler, G.K., 1996. Calcium modulation of adrenocorticotropin levels in women--a clinical research center study. J. Clin. Endocrinol. Metab. 81, 932–936. https://doi.org/10.1210/jcem.81.3.8772553

Impheng, H., Lemmers, C., Bouasse, M., Legros, C., Pakaprot, N., Guérineau, N.C., Lory, P., Monteil, A., 2021. The sodium leak channel NALCN regulates cell excitability of pituitary endocrine cells. FASEB J. 35. https://doi.org/10.1096/fj.202000841RR

Isaac, R., Raymond, J.-P., Rainfray, M., Ardaillou, R., 1984. Effects of an acute calcium load on plasma ACTH, cortisol, aldosterone and renin activity in man. Acta Endocrinol. (Copenh.) 105, 251–257. https://doi.org/10.1530/acta.0.1050251

Kato, M., Hattori, M.A., Suzuki, M., 1988. Inhibition by extracellular Na^+ replacement of GRF-induced GH secretion from rat pituitary cells. Am. J. Physiol.-Endocrinol. Metab. 254, E476–E481. https://doi.org/10.1152/ajpendo.1988.254.4.E476

Kayano, T., Sasaki, Y., Kitamura, N., Harayama, N., Moriya, T., Dayanithi, G., Verkhratsky, A., Shibuya, I., 2019. Persistent Na+ influx drives L-type channel resting Ca2+ entry in rat melanotrophs. Cell Calcium 79, 11–19. https://doi.org/10.1016/j.ceca.2019.02.001

Kretschmannova, K., Kucka, M., Gonzalez-Iglesias, A.E., Stojilkovic, S.S., 2012. The Expression and Role of Hyperpolarization-Activated and Cyclic Nucleotide-Gated Channels in Endocrine Anterior Pituitary Cells. Mol. Endocrinol. 26, 153–164. https://doi.org/10.1210/me.2011-1207

Kucka, M., Kretschmannova, K., Murano, T., Wu, C.-P., Zemkova, H., Ambudkar, S.V., Stojilkovic, S.S., 2010. Dependence of Multidrug Resistance Protein-Mediated Cyclic Nucleotide Efflux on the Background Sodium Conductance. Mol. Pharmacol. 77, 270–279. https://doi.org/10.1124/mol.109.059386

Kučka, M., Kretschmannová, K., Stojilkovic, S.S., Zemková, H., Tomić, M., 2012. Dependence of Spontaneous Electrical Activity and Basal Prolactin Release on Nonselective Cation Channels in Pituitary Lactotrophs. Physiol. Res. 267–275. https://doi.org/10.33549/physiolres.932301

Kwiecien, R., Hammond, C., 1998. Differential Management of Ca^{2+} Oscillations by Anterior Pituitary Cells: A Comparative Overview. Neuroendocrinology 68, 135–151. https://doi.org/10.1159/000054360

Lee, S.-Y., Vuong, T.A., Wen, X., Jeong, H.-J., So, H.-K., Kwon, I., Kang, J.-S., Cho, H., 2019. Methylation determines the extracellular calcium sensitivity of the leak channel NALCN in hippocampal dentate granule cells. Exp. Mol. Med. 51, 1–14. https://doi.org/10.1038/s12276-019-0325-0

Liang, Z., Chen, L., McClafferty, H., Lukowski, R., MacGregor, D., King, J.T., Rizzi, S., Sausbier, M., McCobb, D.P., Knaus, H., Ruth, P., Shipston, M.J., 2011. Control of hypothalamic–pituitary–adrenal stress axis activity by the

713 intermediate conductance calcium-activated potassium channel, SK4. J.
714 Physiol. 589, 5965–5986. https://doi.org/10.1113/jphysiol.2011.219378

715 Lu, B., Su, Y., Das, S., Liu, J., Xia, J., Ren, D., 2007. The Neuronal Channel
716 NALCN Contributes Resting Sodium Permeability and Is Required for Normal
717 Respiratory Rhythm. Cell 129, 371–383.
718 https://doi.org/10.1016/j.cell.2007.02.041

719 Lu, B., Zhang, Q., Wang, H., Wang, Y., Nakayama, M., Ren, D., 2010.
720 Extracellular Calcium Controls Background Current and Neuronal Excitability
721 via an UNC79-UNC80-NALCN Cation Channel Complex. Neuron 68, 488–499.
722 https://doi.org/10.1016/j.neuron.2010.09.014

723 Lussier, B.T., French, M.B., Moor, B.C., Kraicer, J., 1991. Free Intracellular
724 Ca2+ Concentration and Growth Hormone (GH) Release from Purified Rat
725 Somatotrophs, III. Mechanism of Action of GH-Releasing Factor and
726 Somatostatin*. Endocrinology 128, 592–603. https://doi.org/10.1210/endo-128-
727 1-592

728 Lutas, A., Lahmann, C., Soumillon, M., Yellen, G., 2016. The leak channel
729 NALCN controls tonic firing and glycolytic sensitivity of substantia nigra pars
730 reticulata neurons. eLife 5, e15271. https://doi.org/10.7554/eLife.15271

731 Mollard, P., Schlegel, W., 1996. Why are endocrine pituitary cells excitable?
732 Trends Endocrinol. Metab. 7, 361–365. https://doi.org/10.1016/S1043-
733 2760(96)00186-5

734 Naumov, A.P., Herrington, J., Hille, B., 1994. Actions of growth-hormone-
735 releasing hormone on rat pituitary cells: intracellular calcium and ionic currents.
736 Pflugers Arch. Eur. J. Physiol. 427, 414–421.
737 https://doi.org/10.1007/BF00374255

738 Philippart, F., Khaliq, Z.M., 2018. Gi/o protein-coupled receptors in dopamine
739 neurons inhibit the sodium leak channel NALCN. eLife 7, e40984.
740 https://doi.org/10.7554/eLife.40984

741 Protze, S.I., Liu, J., Nussinovitch, U., Ohana, L., Backx, P.H., Gepstein, L.,
742 Keller, G.M., 2017. Sinoatrial node cardiomyocytes derived from human
743 pluripotent cells function as a biological pacemaker. Nat. Biotechnol. 35, 56–68.
744 https://doi.org/10.1038/nbt.3745

745 Ren, D., 2011. Sodium Leak Channels in Neuronal Excitability and Rhythmic
746 Behaviors. Neuron 72, 899–911. https://doi.org/10.1016/j.neuron.2011.12.007

747 Rorsman, P., Ashcroft, F.M., 2018. Pancreatic β-Cell Electrical Activity and
748 Insulin Secretion: Of Mice and Men. Physiol. Rev. 98, 117–214.
749 https://doi.org/10.1152/physrev.00008.2017

750 Sankaranarayanan, S., Simasko, S.M., 1996. A role for a background sodium
751 current in spontaneous action potentials and secretion from rat lactotrophs. Am.
752 J. Physiol.-Cell Physiol. 271, C1927–C1934.
753 https://doi.org/10.1152/ajpcell.1996.271.6.C1927

Shi, Y., Abe, C., Holloway, B.B., Shu, S., Kumar, N.N., Weaver, J.L., Sen, J., Perez-Reyes, E., Stornetta, R.L., Guyenet, P.G., Bayliss, D.A., 2016. Nalcn Is a "Leak" Sodium Channel That Regulates Excitability of Brainstem Chemosensory Neurons and Breathing. J. Neurosci. 36, 8174–8187. https://doi.org/10.1523/JNEUROSCI.1096-16.2016

Simasko, S.M., 1994. A background sodium conductance is necessary for spontaneous depolarizations in rat pituitary cell line GH3. Am. J. Physiol.-Cell Physiol. 266, C709–C719. https://doi.org/10.1152/ajpcell.1994.266.3.C709

Stojilkovic, S.S., 2006. Pituitary cell type-specific electrical activity, calcium signaling and secretion. Biol. Res. 39. https://doi.org/10.4067/S0716-97602006000300004

Stojilkovic, S.S., Kretschmannova, K., Tomić, M., Stratakis, C.A., 2012. Dependence of the Excitability of Pituitary Cells on Cyclic Nucleotides: Cyclic nucleotides and excitability of pituitary cells. J. Neuroendocrinol. 24, 1183–1200. https://doi.org/10.1111/j.1365-2826.2012.02335.x

Stojilkovic, S.S., Tabak, J., Bertram, R., 2010. Ion Channels and Signaling in the Pituitary Gland. Endocr. Rev. 31, 845–915. https://doi.org/10.1210/er.2010-0005

Stojilkovic, S.S., Zemkova, H., Van Goor, F., 2005. Biophysical basis of pituitary cell type-specific Ca2+ signaling–secretion coupling. Trends Endocrinol. Metab. 16, 152–159. https://doi.org/10.1016/j.tem.2005.03.003

Swayne, L.A., Mezghrani, A., Varrault, A., Chemin, J., Bertrand, G., Dalle, S., Bourinet, E., Lory, P., Miller, R.J., Nargeot, J., Monteil, A., 2009. The NALCN ion channel is activated by M3 muscarinic receptors in a pancreatic β-cell line. EMBO Rep. 10, 873–880. https://doi.org/10.1038/embor.2009.125

Tomić, M., Kucka, M., Kretschmannova, K., Li, S., Nesterova, M., Stratakis, C.A., Stojilkovic, S.S., 2011. Role of nonselective cation channels in spontaneous and protein kinase A-stimulated calcium signaling in pituitary cells. Am. J. Physiol.-Endocrinol. Metab. 301, E370–E379. https://doi.org/10.1152/ajpendo.00130.2011

Tsaneva-Atanasova, K., Sherman, A., van Goor, F., Stojilkovic, S.S., 2007. Mechanism of Spontaneous and Receptor-Controlled Electrical Activity in Pituitary Somatotrophs: Experiments and Theory. J. Neurophysiol. 98, 131–144. https://doi.org/10.1152/jn.00872.2006

Vela, J., Pérez-Millán, M.I., Becu-Villalobos, D., Díaz-Torga, G., 2007. Different kinases regulate activation of voltage-dependent calcium channels by depolarization in GH3 cells. Am. J. Physiol.-Cell Physiol. 293, C951–C959. https://doi.org/10.1152/ajpcell.00429.2006

Yeh, S.-Y., Huang, W.-H., Wang, W., Ward, C.S., Chao, E.S., Wu, Z., Tang, B., Tang, J., Sun, J.J., Esther van der Heijden, M., Gray, P.A., Xue, M., Ray, R.S., Ren, D., Zoghbi, H.Y., 2017. Respiratory Network Stability and Modulatory Response to Substance P Require Nalcn. Neuron 94, 294-303.e4. https://doi.org/10.1016/j.neuron.2017.03.024

Zemkova, H., Tomić, M., Kucka, M., Aguilera, G., Stojilkovic, S.S., 2016. Spontaneous and CRH-Induced Excitability and Calcium Signaling in Mice Corticotrophs Involves Sodium, Calcium, and Cation-Conducting Channels. Endocrinology 157, 1576–1589. https://doi.org/10.1210/en.2015-1899

Figure 1

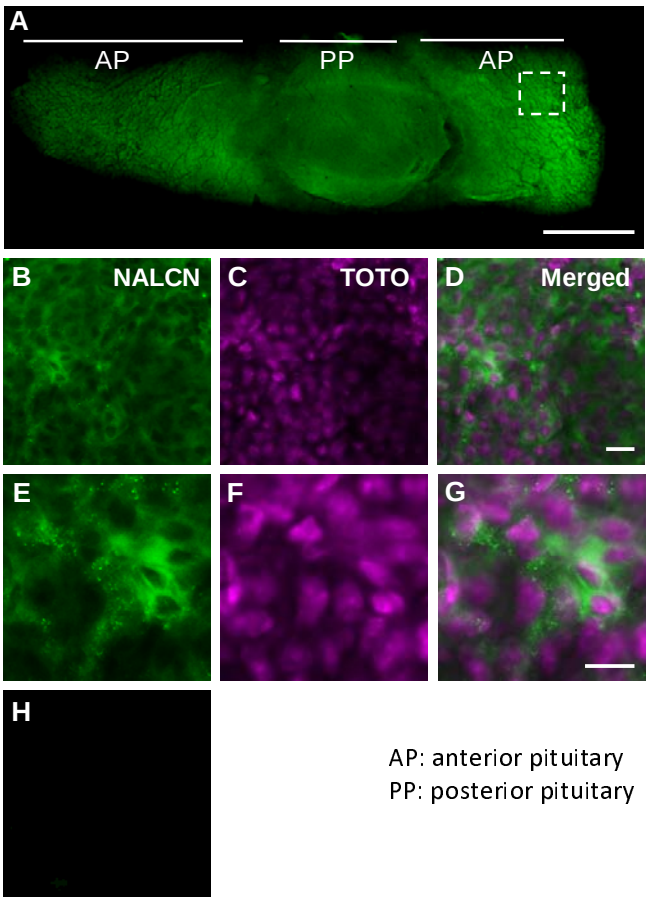

Figure 1. The NALCN ion channel is expressed in mouse pituitary gland. Immunofluorescence staining revealed the presence of NALCN protein in mouse pituitary gland (n=3). NALCN is shown in green. TOTO-3 (shown in magenta) was used to visualise cellular nucleic acids. **A)** Transverse section of a pituitary gland under 10X magnification excited with 488 nm light to detect NALCN immunofluorescence. **B)** NALCN visualisation in the area defined by dashed square in A. **C)** Toto-labelled nucleic acid in the same area. **D)** Merged image from B and C. B, C and D are under 20X magnification. **E-G)** are under higher digital magnification using confocal microscopy. **H)** Negative control tissue for which the primary anti NALCN antibody was omitted. The scale bars indicate 500 µm in panel A, and 20 µm in panels D and G.

Figure 2

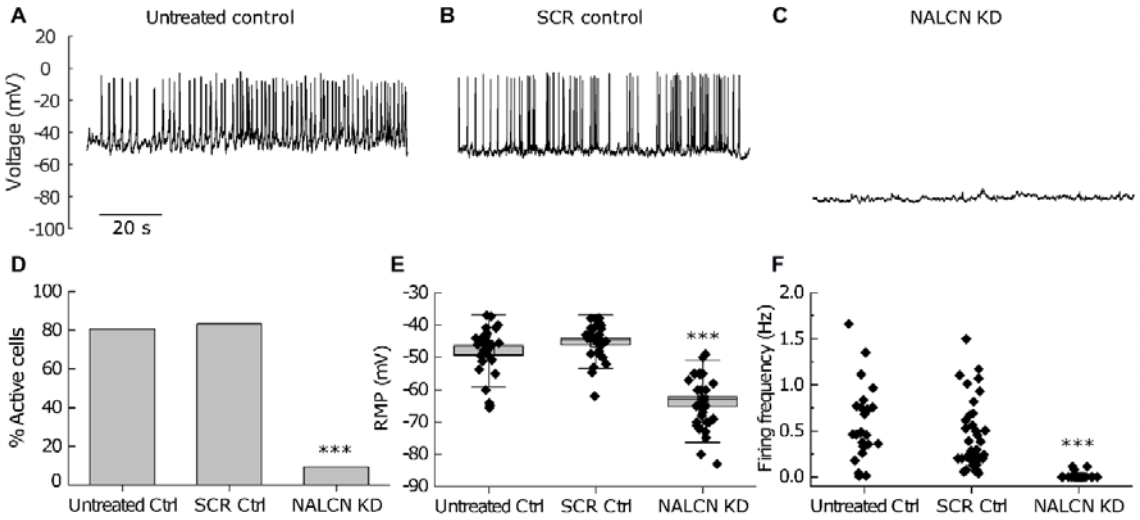

Figure 2. Knock-down of NALCN silences electrical activity of primary murine pituitary cells. Representative traces of spontaneous firing activity from **A)** an untreated and **B)** a scramble control (SCR Ctrl) pituitary cell. **C)** Representative trace of electrical activity in a NALCN knockdown (NALCN KD) pituitary cell. **D)** Percentages of active and silent cells in untreated control, SCR Ctrl and NALCN KD pituitary cells. **E)** Resting membrane potential of untreated control, SCR Ctrl and NALCN KD pituitary cells (data presented as mean ± SD, untreated control: -47.6 ± 7.6 mV, n=31 vs SCR control: -45 mV ± 5.8 mV, n=30, p>0.1; NALCN KD: -63.6 ± 8.5 mV, n=31 vs SCR Ctrl and untreated control: $p < 0.001$, one-way ANOVA with Bonferroni correction), the box represents the standard error, the whiskers represent standard deviation (SD). **F)** Distribution of firing frequency between untreated Ctrl, SCR Ctrl and NALCN KD cells over a course of 600 seconds (data presented as mean ± SD, NALCN KD: 0 Hz, n= 31 vs SCR Ctrl: 0.5 ± 0.4 Hz, n= 25 and vs untreated Ctrl: 0.7 ± 0.6 Hz, n= 25, $p < 0.001$; SCR Ctrl vs untreated Ctrl: $p > 0.1$, one-way ANOVA with Bonferroni correction). Only three out of 31 NALCN KD cells exhibited firing activity, which occurred at a lower frequency (0.1 ± 0.02 Hz) relative to the

867 untreated and SCR controls. In each graph, triple asterisks (***) represents p <
868 0.001.
869
870
871
872
873 **Figure 3**
874
875 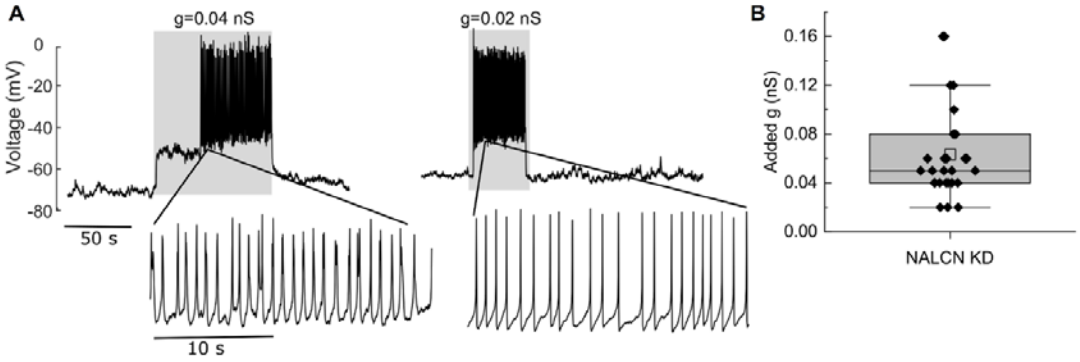
876
877
878
879
880
881
882
883 **Figure 3. Addition of nonselective cationic conductance restores firing**
884 **activity in silent NALCN KD pituitary cells. A)** Two representative voltage
885 traces of silent NALCN Knock-down (NALCN KD) pituitary cells. Firing activity
886 was restored once the nonselective cationic conductance (g) was increased by
887 a very minute amount, such as 0.02 (right panel, the cell started silent and then
888 discharges APs mid-way) or 0.04 nS (left panel). The cells immediately returned
889 to a silent and hyperpolarised state after removal of the added conductance. **B)**
890 The distribution of added conductance (g) values required for restoring the firing
891 activity in NALCN KD pituitary cells. Median: 0.05 nS, n=28.
892
893
894
895
896
897
898
899
900
901

Figure 4

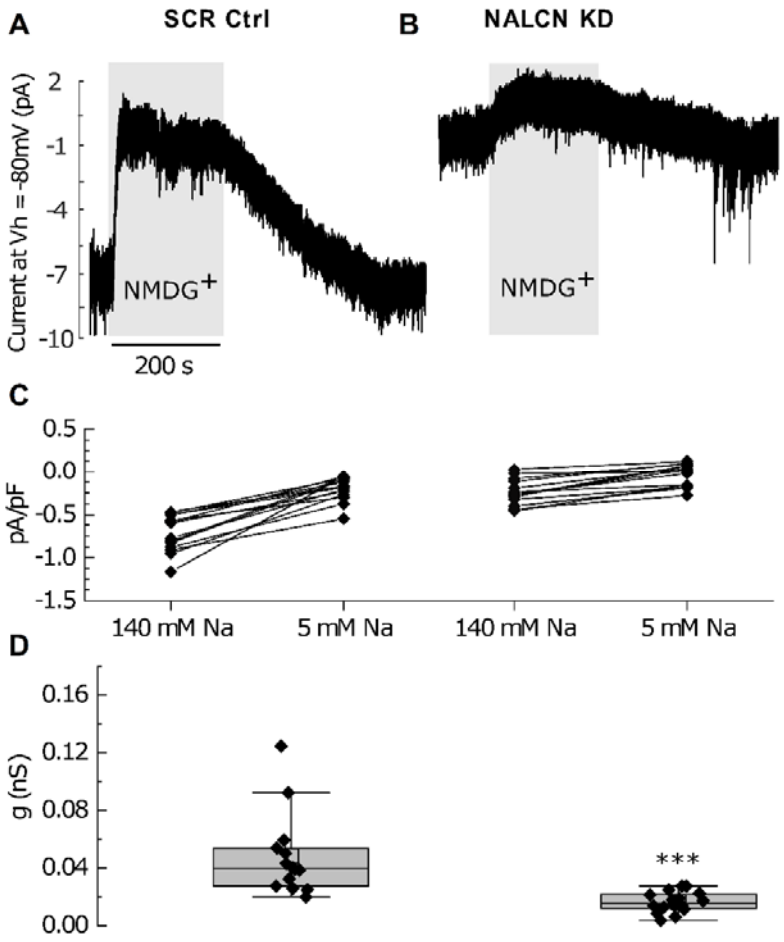

Figure 4. NALCN contributes most of the inward Na^+ leak conductance in endocrine anterior pituitary cells. A) Representative trace of an inward Na^+ leak current (V_h=-80 mV) in a SCR Ctrl pituitary cell as revealed by the substitution of extracellular Na^+ with $NMDG^+$. **B)** Representative trace of an inward leak current in a NALCN KD pituitary cell as revealed by the substitution of extracellular Na^+ with $NMDG^+$. **C)** The density of the inward Na^+ leak current

in NALCN KD cells was significantly reduced compared to SCR Ctrl (data presented as mean ± SD, SCR Ctrl: -0.72 ± 0.2 pA/pF (-5.2 ± 1.9 pA), n=15; NALCN KD: -0.19 ± 0.13 pA/pF (-1.5 ± 0.9 pA), n=16; p< 0.001, *t*-test). **D)** The background Na^+ conductance was more strongly reduced by Na^+ removal in control cells than in NALCN KD cells (data represented as Median ± interquartile, SCR control: 0.045 ± 0.02 nS, n = 16; NALCN KD: 0.015 ± 0.01 nS , n = 15; p < 0.001, Mann Whitney test).

Figure 5

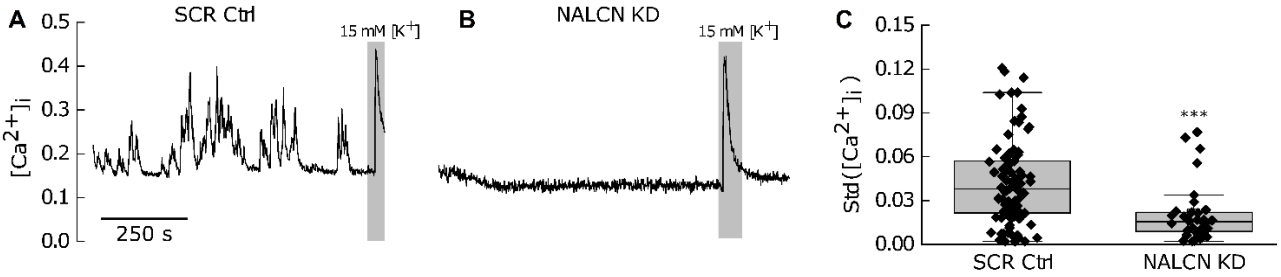

Figure 5. NALCN KD impacts on intracellular Ca^{2+} transients.

A) Representative trace of intracellular Ca^{2+} oscillations in an SCR control pituitary cell. The final peak in each graph represents the extracellular K^+ (15 mM)-induced rise in $[Ca^{2+}]_i$, which was used to check cell viability. **B)** A representative trace of $[Ca^{2+}]_i$ in a NALCN KD pituitary cell. **C)** The standard deviation of each $[Ca^{2+}]_i$ trace was calculated and statistical analysis revealed a significant alteration of $[Ca^{2+}]_i$ oscillations between the two groups (SCR Ctrl: median= 0.04, n = 90 from 4 mice; NALCN KD: median= 0.015, n = 36 from 4 mice; p < 0.001, Mann Whitney test). Box: inter-quartile, Whiskers: range, excluding outliers, Central line: median.

Figure 6

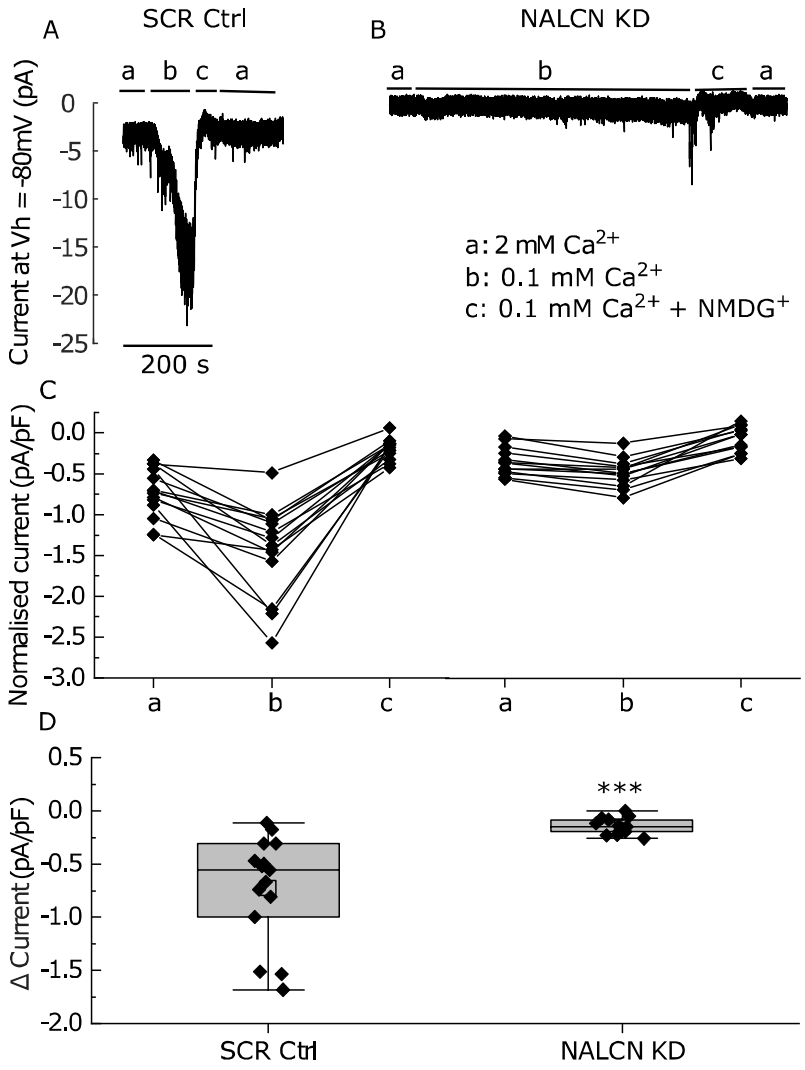

Figure 6. NALCN is sensitive to the changes in extracellular Ca^{2+} level. **A)** Representative trace of inward leak current in a SCR control pituitary cell. Reducing extracellular Ca^{2+} significantly increased the inward leak current over a time-course of 20 to 200 seconds (b). Subsequent replacement of extracellular Na^{+} with $NMDG^{+}$ strongly reduced the holding inward leak current (c). **B)** Representative trace of the inward leak current in a NALCN KD pituitary cell; lowering the extracellular Ca^{2+} resulted in a small rise in the inward leak

current (b, applied for a longer time to rule out any further change in current). Subsequent replacement of extracellular Na^+ with $NMDG^+$ reduced this inward current (c). **C)** Normalised inward leak current in 2mM Ca^{2+} (a), 0.1 mM Ca^{2+} (b), and 0.1 mM Ca^{2+} + $NMDG^+$ (c) in SCR control (left) and NALCN KD cells (right). **D)** The overall rise in inward leak current after reducing extracellular Ca^{2+} in SCR control cells (left), compared to NALCN KD cells (right). Median ± interquartile in SCR Control: −0.6 ± 0.6 pA/pF, n = 13; NALCN KD: −0.13 ± 0.1 pA/pF, n = 13, $p < 0.001$, Mann Whitney test. Box: inter-quartile, Whiskers: range excluding outliers, Central line: median.